DOI: 10.1007/s11099-016-0185-y PHOTOSYNTHETICA 54 (3): 422-429, 2016

Chlorophyll *a* fluorescence analysis of high-yield rice (*Oryza sativa* L.) LYPJ during leaf senescence

Y.W. WANG [*], C. XU [*], C. F. LV[*], M. WU [*, **], X.J. CAI [*], Z.T. LIU [*], X.M. SONG [*], G.X. CHEN [*,+], and C.G. LV [***]

Jiangsu Key Laboratory of Biodiversity and Biotechnology, Life Sciences College, Nanjing Normal University, Nanjing 210023, China[*]
Zijin College, Nanjing University of Science and Technology, Nanjing 210023, China[**]
Institute of Food and Crops, Jiangsu Academy of Agricultural Sciences, Nanjing 210014, China[***]

Abstract

Photosystem II (PSII) photochemistry was examined by chlorophyll (Chl) *a* fluorescence analysis in high-yield rice LYPJ flag leaves during senescence. Parameters deduced from the JIP-test showed that inhibition of the donor side of PSII was greater than that of the acceptor side in hybrid rice LYPJ. The natural senescence process was accompanied by the increased inactivation of oxygen-evolving complex (OEC) and a lower total number of active reaction centers per absorption. It indicated that the inhibition of electron transport caused by natural senescence might be caused partly by uncoupling of the OEC and/or inactivation of PSII reaction centers. Chl fluorescence parameters analyzed in this study suggested that energy dissipation was enhanced in order to protect senescent leaves from photodamage. Nevertheless, considerably reduced PSI electron transport activity was observed at the later senescence. Thus, natural senescence inhibited OEC–PSII electron transport, but also significantly limited the PSII–PSI electron flow.

Additional key words: JIP-test; natural senescence; PSII efficiency; thylakoid membrane.

Introduction

Rice (*Oryza sativa* L.) is one of the most important cereal crops, cultivated in Asia, Africa, and Latin America (Wu *et al*. 2014). According to Jiao *et al*. (2003), hybrid rice might suffer from early or premature senescence during the late developmental stages. Photosynthesis at a grain-filling period, which coincided with the occurrence of flag leaf senescence in hybrid rice plants, contributed approximately by 60–100% of carbon in grains originating from CO_2 assimilation (Wang *et al*. 2014). Therefore, the rate of leaf senescence (starts from full expansion of flag leaves) was closely related to the grain filling (Panda and Sarkar 2013). The effect of natural senescence on photosynthetic performance was foreseen by alterations in the structure and function of the chloroplasts, which resulted in the decreased photosynthetic rate (Panda and Sarkar 2013, Wang *et al*. 2014).

Chlorophyll (Chl) *a* fluorescence analysis has been shown to be a noninvasive, powerful, and reliable method to assess the variation in the phenomenological and biophysical expressions of PSII in different species to different environmental conditions, such as light intensity (Brestič *et al*. 2014), salinity (Xia *et al*. 2004), temperature (Stefanov *et al*. 2011, Sharma *et al*. 2014), drought (Boureima *et al*. 2012), toxic metals (Kumar *et al*. 2014), nutrient deficiency (Kalaji *et al*. 2014, Osório *et al*. 2014), UV-B radiation (Wang *et al*. 2010a), and chemical influences (Mohapatra *et al*. 2010, Qiu *et al*. 2013, Kreslavski *et al*. 2014). Fast measurement of the F_v/F_m

---

Received 14 May 2015, *accepted* 5 November 2015, *published as online-first* 11 November 2015.

[+]Corresponding author; fax: +862585891236, e-mail: gxchennjnu@hotmail.com

Abbreviations: Chl – chlorophyll; CS – cross section; DF – the total driving force for photosynthesis of the observed system; F_0 – fluorescence intensity at 50 μs; F_J – fluorescence intensity at the J-step (at 2 ms); F_I – fluorescence intensity at the I-step (at 30 ms); F_M – maximal fluorescence intensity; F_v/F_m – maximum photochemical efficiency of PSII; OEC – oxygen-evolving complex; P680 – primary electron donor in PSII; PI_{cs} – the performance index on cross section basis at different times; PI_{tot} – the potential for energy conservation from photons absorbed by PSII to the reduction flux (RE) of PSI end acceptors; PQ – plastoquinone; RC – PSII reaction center; t_{FM} – time to reach F_M.

Acknowledgements: This research was supported by the National Natural Science Foundation of China (No. 31271621), Natural Science Foundation of the Jiangsu Province, China (No. 11KJA180001), the Priority Academic Program Development of Jiangsu Higher Education Institutions (PAPD), and NSFC for Talents Training in Basic Science (J1103507, J1210025).

ratio was the most common parameter, but F_v/F_m was shown to be nonspecific and often insensitive (Boureima *et al.* 2012, Stirbet and Govindjee 2011). Based on the energy flux theory in photosynthetic membranes, an analysis of the fast OJIP fluorescence rise in Chl *a* fluorescence induction has been developed, referred as the "JIP-test" (Strasser and Strasser 1995). Such an analysis took into account the different steps and phases of the transient with the redox states of PSII. From another aspect, it could also extend our insight and realize the efficiencies of electron transfer through the intersystem chain to the end electron acceptors at the PSI acceptor side, concomitantly (Tsimilli-Michael and Strasser 2008, Pollastrini *et al.* 2014). However, it is worthwhile to mention that the JIP-test is not the only way of evaluation of the OJIP curves and that the curves can be affected by many factors (Lazár 2006). Most of literature on changes in Chl *a* fluorescence in rice were mainly performed at a vegetative stage under different abiotic stresses (Panda and Sarkar 2013, Chhotaray *et al.* 2014, Li *et al.* 2014). Detailed information on hybrid rice during natural senescence processes is not available on energy absorption, utilization, and dissipation of excess excitation energy using Chl *a* fluorescence technique after full expansion of flag leaves.

In addition to agronomic and biotechnological strategies, improvement of weakness in hybrid rice through breeding and molecular tools is in progress (Wu *et al.* 2013, Chen *et al.* 2014). Most of the methods on evaluation of early or premature senescence would be complex and time-consuming under field conditions. Due to the ease-of-use, time-saving, and noninvasiveness of Chl *a* fluorescence measurement, it could be developed into an indirect screening indicator for hybrid rice breeding under field conditions (Hsu 2007). On this background, we analyzed the changes in PSII photochemistry in flag leaves of high-yield rice LYPJ during senescence by means of parameters derived from the fast Chl *a* fluorescence records. We assumed that different developmental periods would be accompanied by different effects on photochemical processes.

Materials and methods

Plant material: Field experiments were performed with the cultivar LYPJ of rice (*O. sativa* L.), which was one of the most cultivated super high-yield hybrid rice variety in China, at the experimental fields of the Institute of Agricultural Sciences of Jiangsu Nanjing, China. The total N fertilizer was applied at 225 kg per 667 m^2, with an N:P:K ratio of 1:0.6:0.6 (Yu *et al.* 2013). During the period from 15 August (first flag leaf expansion) to 25 September (the harvest time) in 2013, the sampling took place in the morning (09:30–10:30 h) on sunny days at approximately one-week intervals.

Analysis of fast Chl *a* fluorescence induction dynamics: Chl *a* fluorescence of leaves was measured with a pocket fluorometer (*Handy PEA*, *Hansatech*, UK) by referring to methods of Strasser *et al.* (1995). Leaves were dark-adapted for approximately 30 min prior to measurements and then exposed to red light of 650 nm through LED at excitation irradiance of 3,000 μmol(photon) m^{-2} s^{-1} with a duration of 800 ms. The experiment was carried out in triplicate and each replicate contained ten leaves of different plants. This experiment was repeated four times. Statistical testing of normality of data distribution was performed according to the method of Lazár and Nauš (1998). The parameters were calculated as mentioned in Table 1 (Lazár 2006, Shen *et al.* 2015).

Protein immunoblot analysis: Rice leaves were washed with cold water and used for extraction of thylakoid membranes as described by Timperio *et al.* (2007) and processed as described by D'Amici *et al.* (2008). Separation and solubilization of thylakoid membrane complexes were performed according to the method of Kügler *et al.* (1997). The isolated thylakoid membrane suspension was pretreated with loading buffer containing 5% SDS, 30 mM mercaptoethanol, 5% sucrose, 2 mM EDTA, 0.02% Bromophenol Blue, and 125 mM Tris-HCl (pH 6.8), and boiled for 5 min. For protein immunoblot analysis, isolated thylakoid protein samples with the same amount of Chl were first separated by 12 % SDS-PAGE, then transferred to PVDF membranes and immunoblotted with various antibodies (*Agrisera*, Sweden). Antibodies were detected using a chemiluminescence detection system (*ECL*, *Qiagen*).

Results

OJIP fluorescence rise kinetics: The OJIP fluorescence rise showed characteristic difference at each phase after full expansion of the flag leaves (O-J, J-I, and I-P phase) (Fig. 1*A*). The O-J phase showed some changes, whereas the intensity in the phases of J-I and I-P significantly decreased. Significant difference was observed on 14 d after full expansion (DAE) of the flag leaves. During this period, an increase in F_0 (50 μs), F_J (2 ms), F_I (30 ms), but a decrease in F_M (at t_{FM}) were observed. F_0 increased by 6.5% on 14 DAE of the flag leaves, with simultaneous 8.2% rise in F_J, 0.8% in F_I, and 6.4% reduction in F_M. Analysis of the fluorescence transients revealed that the major effects of natural senescence for hybrid rice LYPJ plants occurred in the I-P phase. There was reduction

Table 1. Formulae and definitions of the selected JIP-test fluorescence parameters used in the present study. Subscript "0" (or "o" when written after another subscript) indicates that the parameter refers to the onset of illumination, when all RCs are assumed to be open. The parameters were calculated as mentioned in Lazár (2006) and Shen *et al.* (2015).

Terms and formulae	Illustrations
$V_J = (F_J–F_0)/(F_M–F_0)$	Relative variable fluorescence at the phase J of the fluorescence induction curve
$V_I = (F_I–F_0)/(F_M–F_0)$	Relative variable fluorescence at the phase I of the fluorescence induction curve
$V_K= (F_K–F_0)/(F_M–F_0)$	Relative variable fluorescence at the phase K of the fluorescence induction curve
$W_K= (F_K–F_0)/(F_J–F_0)$	Represent the damage to oxygen evolving complex OEC
V_K/ V_J	Relative measure of inactivation of OEC
$S_M = Area/F_V$	Normalized total complementary area above the OJIP transient
$Sum\ K = K_P + K_N$	The sum of photochemical rate constant K_P and nonphotochemical rate constant K_N
K_N	The nonphotochemical de-excitation rate constant in the excited antennae for nonphotochemistry
K_P	The photochemical de-excitation rate constant in the excited antennae of energy fluxes for photochemistry
$ABS/RC = (M_0/V_J)/[1– (F_0/F_M)]$	Light absorption flux (for PSII antenna chlorophylls) per reaction center (RC)
$DI_0/RC = ABS/RC–TR_0/RC$	Dissipation energy flux per PSII reaction center (RC) (at t = 0)
$ET_0/RC = (M_0/V_J) \times (1 – V_J)$	Maximum electron transport flux (further than Q_A^-) per PSII reaction center (RC) (at t = 0)
$TR_0/RC = (M_0/V_J)$	Trapped (maximum) energy flux (leading to Q_A reduction) per reaction center (RC) (at t = 0)
$RE_0/RC = M_0\ (1/V_J)\ (1 – V_I)$	Electron flux reducing end electron acceptors at the PSI acceptor side per RC
$\varphi P_0 = TR_0/ABS = F_V/F_M = [1– (F_0/F_M)]$	The maximum quantum yield of primary photochemistry
$\varphi E_o = ET_0/ABS = [1 – (F_0/F_M)] \times (1–V_J)$	The quantum yield of electron transport
$\Psi_0 = 1 – V_J$	The efficiency with which a trapped exaction can move an electron into the electron transport chain further than Q_A
$\varphi D_0 = DI_0/ABS = 1 – \varphi P_0 = (F_0/F_M)$	Thermal dissipation quantum yield
$\delta R_0 = (1 – V_I)/(1 – V_J)$	Efficiency/probability with which an electron from the intersystem electron carriers moves to reduce end electron acceptors at the PSI acceptor side
$\varphi R_0 = \varphi P_0\ \ \psi E_0\ \ \delta R_0$	The quantum yield of reduction of end electron acceptors of PSI
$ABS/CS_m = F_M$	Absorption flux of photons per cross section, approximated by F_M
$TR_0/CS_m = \varphi p_0 \times (ABS/CS_m)$	Phenomenological fluxes for trapping per cross section, approximated by F_M
$ET_0/CS_m = \varphi E_0 \times (ABS/CS_m)$	Potential electron transport per cross section, approximated by F_M
$DI_0/CS_m = (ABS/CS_m) – (TR_0/CS_m)$	Dissipation per cross section, approximated by F_M
$PI_{ABS} = (RC/ABS) \times [\varphi P_0/(1 – \varphi P_0)] \times [\psi_0/(1 – \psi_0)]$	The performance index on absorption basis

in the net Chl *a* content of leaves with onset of senescence (*see* Wang *et al.* 2014), and this might affect the fluorescence peaks.

A significant K rise was noticed in the transients on 35 DAE in the flag leaves. It has been also noticed that the phase K was caused by an inhibition of electron transfer to the secondary electron donor of PSII, which was due to a damaged oxygen-evolving complex (OEC) (Holland *et al.* 2014). We assayed the accumulation of subunits of OEC by immunoblot analysis. Immunoblotting revealed that the PsbO, PsbP, and PsbQ slightly declined in parallel on 21 DAE but notably declined during the next days (Fig. 1*B*).

The donor and acceptor side of PSII: In order to study further the effect of natural senescence on the electron transport at the donor side of PSII in this cultivar, two parameters, V_K and W_K, were measured. Natural senescence did not result in obvious changes of V_K and W_K, till 14 DAE (Fig. 2*A*,*B*). When the natural senescence occurred on 21 DAE, V_K went up significantly. Moreover, W_K (as a relative measure of inactivation of OEC) significantly increased as the flag leaves reached senescence, which was found directly proportional to the age of the leaves.

Fig. 2*C* demonstrated the changes in the acceptor side of PSII. Sum K showed more or less a decreasing trend after full expansion of the flag leaves. The net rate of PSII closure (M_o) increased significantly after full expansion of the flag leaves, confirming that there was an inhibition on the acceptor side, in electron transport between Q_A and Q_B. A similar trend was recorded in K_p, which reached its minimum on 35 DAE exhibiting 27% decrease. The non-photochemical de-excitation rate constant in the excited antennae for nonphotochemistry gradually increased.

Analyses of the JIP test showed that V_k increased by 45.4% at 21 DAE and 172 % at 35 DAE. W_k increased by 19.4% and 76.6 % on 21 and 35 DAE, respectively, during the senescence stage. The V_J showed no change at 21 DAE but it decreased by 11.4% at 35 DAE during the senescence stage (Fig. 2*C*). The V_I decreased by 7.8% at

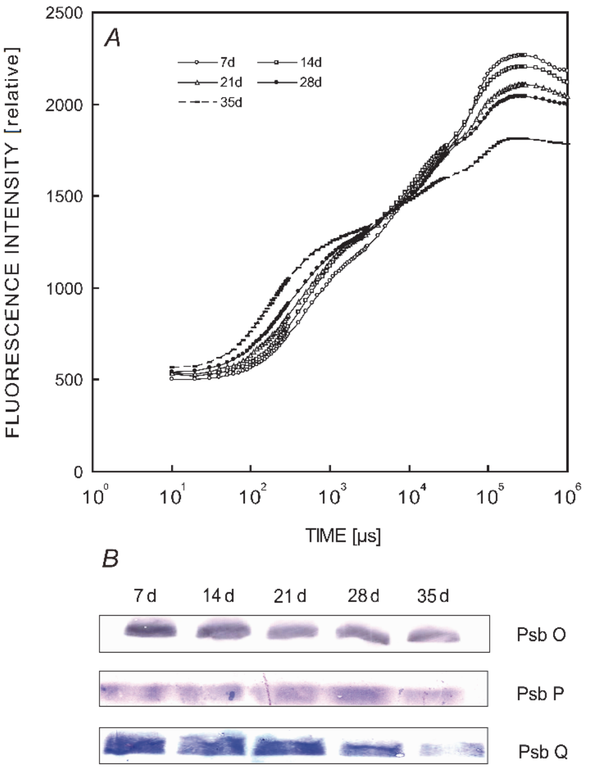

Fig. 1. Changes in chlorophyll fluorescence transient of leaf senescence of super high-yield LYPJ hybrid rice (*A*). Immunoblot with antibodies against oxygen-evolving complex–associated protein of thylakoid isolated from leaves after full expansion of flag leaves (*B*). Each lane was loaded with amount of pigment-protein complexes corresponding to 2 µg of Chl.

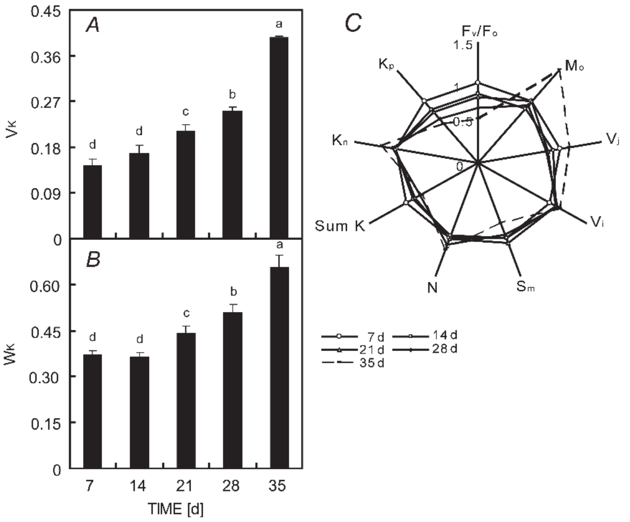

Fig. 2. Changes in PSII donor side (*A*, *B*) and acceptor side (*C*) during leaf senescence of high-yield LYPJ hybrid rice. Data are means with error bars indicating SD (n = 10). *Different small letters* indicate significant differences at $P<0.05$.

21 DAE and 11.4% at 35 DAE. Hence, the inhibition of the donor side of PSII was greater than that of the acceptor side. This finding indicated that the electron transfer capability of both donor and the acceptor side of the PSII reaction centre was significantly altered by natural senescence.

The amount of PSII reaction centers: Natural senescence induced 22% decrease of RC/CS_o, 38% decrease of RC/ABS on 35 DAE (Fig. 3*A*). Reducing the number of active reaction centers of this rice cultivar meant that less energy was used to drive electron transport. Therefore, this energy must be dissipated by nonphotochemical mechanisms.

PSII efficiency and excitation energy dissipation: The quantum yields are shown in Table 2. The values of the maximum quantum yield of primary photochemistry (φP_0), the quantum yield of the electront ransport (φE_0), and the probability that a trapped exciton moves an electron into the electron transport chain beyond Q_A (ψ_0) decreased by 16.3, 25.2, and 15.6%, respectively, on 35 DAE. An apparent increase was found in thermal dissipation quantum yield (φD_0).

The quantum yield of reduction of end electron acceptors of PSI was expressed as φR_0. φR_0 decreased by 61.4% on 35 DAE. The decrease of this parameter was associated with the decrease in IP amplitude (ΔV_{IP})

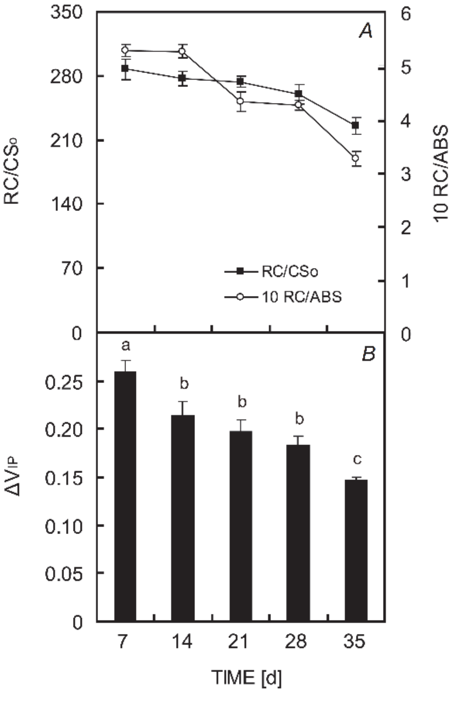

Fig. 3. Changes in the amount of active PSII reaction centers per excited cross section (RC/CS_0) and the total number of active reaction center per absorption (RC/ABS) (*A*), and the content of PSI reaction centers (ΔVIP) (*B*) during leaf senescence of high-yield hybrid rice LYPJ. Vertical bars show standard errors (n = 10). *Different small letters* indicate significant differences at $P<0.05$.

Table 2. Quantum yields and flux ratios, specific energy fluxes per Q_A-reducing PSII centers and phenomenological fluxes during leaf senescence of high-yield LYPJ hybrid rice. *Different letters* in superscript indicate significant differences at $P<0.05$.

Variable		Time after full expansion of flag leaves [d]				
		7	14	21	28	35
Quantum efficiencies	φP_0	0.765 ± 0.009^a	0.736 ± 0.008^b	0.726 ± 0.006^b	0.691 ± 0.011^b	0.636 ± 0.008^c
	φE_0	0.426 ± 0.019^a	0.436 ± 0.007^a	0.449 ± 0.004^a	0.436 ± 0.017^a	0.318 ± 0.015^b
	Ψ_0	0.557 ± 0.011^b	0.593 ± 0.009^a	0.619 ± 0.007^a	0.631 ± 0.012^a	0.499 ± 0.016^c
	φD_0	0.235 ± 0.019^d	0.264 ± 0.017^c	0.274 ± 0.009^c	0.309 ± 0.021^b	0.364 ± 0.031^a
	δR_0	0.176 ± 0.007^a	0.155 ± 0.017^a	0.162 ± 0.014^a	0.156 ± 0.009^b	0.108 ± 0.011^b
	φR_0	0.057 ± 0.006^a	0.054 ± 0.006^a	0.053 ± 0.001^a	0.047 ± 0.003^b	0.022 ± 0.001^c
Specific fluxes	ABS/RC	1.896 ± 0.004^c	1.898 ± 0.004^c	2.346 ± 0.004^b	2.355 ± 0.003^b	3.382 ± 0.0032^a
	DI_0/RC	0.445 ± 0.003^d	0.500 ± 0.003^c	0.638 ± 0.004^b	0.728 ± 0.004^b	1.279 ± 0.0031^a
	ET_0/RC	0.807 ± 0.002^b	0.827 ± 0.002^b	1.056 ± 0.003^a	1.027 ± 0.002^a	1.046 ± 0.002^a
	TR_0/RC	1.4505 ± 0.037^c	1.397 ± 0.031^c	1.708 ± 0.034^b	1.627 ± 0.036^b	2.103 ± 0.031^a
Phenomenological fluxes	ABS/CS_M	$2{,}318 \pm 52^a$	$2{,}288 \pm 59^a$	$2{,}293 \pm 58^a$	$2{,}209 \pm 51^a$	$1{,}959 \pm 50^b$
	TR_0/CS_M	$1{,}773 \pm 47^a$	$1{,}686 \pm 39^b$	$1{,}663 \pm 41^b$	$1{,}525 \pm 49^c$	$1{,}256 \pm 45^c$
	ET_0/CS_M	987 ± 11^a	997 ± 19^a	$1{,}028 \pm 27^a$	963 ± 13^b	631 ± 12^c
	DI_0/CS_M	554 ± 11^d	602 ± 12^c	628 ± 28^c	683 ± 12^b	702 ± 13^a

(Fig. 3*B*). The specific activities per reaction centre (RC) and phenomenological fluxes per cross section (CS_m) were presented in Table 2. The derived specific fluxes per active PSII RC were affected after full expansion of the flag leaves during the senescence stage. Both ABS/RC and TR_0/RC significantly increased under natural senescence. In spite of this, ET_0/RC did not notably differ after full expansion of the flag leaves during the senescence stage, because of the significantly higher DI_0/RC.

The derived phenomenological fluxes per excited leaf sample CS, estimated from F_M, were reduced after full expansion of the flag leaves during the senescence stage (Table 2). Associating with ABS/CS_M, the photons absorbed by antenna molecules slightly decreased during 7–21 DAE, but notably decreased on 28 DAE (Table 2). We noted here that the gradually decreased TR_0/CS_M and increased DI_0/CS_M led to a reduction in ET_0/CS_M in rice after full expansion of the flag leaves.

PSII performance index: The values of performance indices (PI_{tot}, PI_{abs}, PI_{csm}, PI_{cso}) were normalized to those of the 7 DAE old rice plants (Fig. 4). The parameters were used to quantify the PSII behavior and found decreased significantly during natural senescence, but the F_v/F_m ratio showed insignificant variation. Over 21 DAE, the decreases of PI_{abs} and PI_{csm} were much more pronounced compared to other parameters.

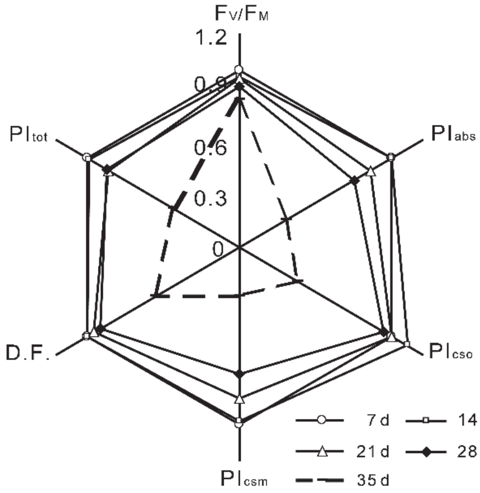

Fig. 4. The total performance index (PI_{tot}), the performance index on absorption basis (PI_{abs}), the performance index on cross section (PI_{csm}, PI_{cso}) of flag leaves during leaf senescence of high yield hybrid rice LYPJ.

Discussion

In our study, V_K and W_K significantly increased after full expansion of the flag leaves during the senescence stage, which further indicated that natural senescence had a negative effect on electron transport at the donor side of PSII (Feng *et al.* 2014). By analyzing key sites in the electron transport chain, we also found that at the beginning of senescence there was no obvious variation in F_v/F_o, M_o, V_J, and V_I parameters. However, significant changes occurred during the later senescence process, indicating a limitation at the acceptor side of PSII (Fig. 2*C*). Hence, we speculate that the inhibition of the donor side was greater than that of the acceptor side. This difference would disturb the electron transport capacity of PSII after full expansion of the flag leaves in LYPJ rice, resulting in a larger imbalance in the ratio of PSII to intersystem transport activities. This phenomenon would accelerate leaf senescence after full expansion of the flag leaves.

The later senescence process was accompanied by the appearance of the K-phase, quantified as the increase in W_K (a partial uncoupling of OEC) (Fig. 2*B*) (Kalachanis and Manetas 2010, Feng *et al.* 2014). In present study, the late occurrence of the K-phase showed that disruption at the acceptor side of PSII did not result in a serious decrease in PSII activity at the beginning of senescence (Table 2). During this period, the increased value of W_K proved that natural senescence in hybrid LYPJ rice caused partial damage of the electron transport from OEC to $P680^+$, but the effect was not strong enough to generate a distinct OKJIP transient, caused by the impairment of a very small part of OEC. This could be confirmed by the variation in amounts of OEC subunits (PsbO, PsbP, and PsbQ) after full expansion of the flag leaves (Fig. 1*B*).

We compared the quantum efficiencies φP_0, φE_0, ψ_0, and φR_0 after full expansion of the flag leaves. The energy dissipation efficiency (φD_0), increased with the aging process due to its direct relationship with the decreased quantum yield of primary photochemistry (φP_0). Hence, we concluded that PSII in hybrid LYPJ rice suffered from some inactivation not only in energy trapping, but also in the electron flow during the senescence stage. Another point of concern was the gradual decrease in the relative amplitude of the I-P phase in rice. There was experimental evidence that I-P phase was related to the events in the vicinity of PSI, mainly the electron flow from PSI to the final electron acceptors (Schansker *et al.* 2005, Kalachanis and Manetas 2010, Hussain and Reigosa 2011). Recently, it has also been proposed that a link between a low value of ΔV_{IP} and a low content of PSI, or a decrease of PSI fraction, are involved in the linear electron flow (Kalachanis and Manetas 2010, Ceppi *et al.* 2012, Holland *et al.* 2014). As shown in Fig. 3*B*, a smaller value of ΔV_{IP} in hybrid LYPJ rice was observed during later senescence process at 28 DAE. The variation was not significant from 14 to 28 DAE, but notably decreased from 28 to 35 DAE. However, the probability of an electron from reduced intermediate carriers to reduce the end acceptor of PSI (δR_o) was lower in hybrid LYPJ rice on 28 DAE during later senescence, indicating that a hindered electron flow along PSII was accompanied with a later hindrance along PSI in this study. It has been suggested that PSII was more susceptible to natural senescence than PSI and a greater decrease in PSII activity was observed during the later senescence process (Panda and Sarkar 2013).

It was of interest to find out if natural senescence could alter the ratio between antenna light-harvesting complex and active PSII reaction centres during the senescence process (Table 2). Then, the increase in ABS/RC reflected that either a fraction of RCs was inactivated or the apparent antenna size increased (Alberta *et al.* 2008, Wang *et al.* 2010b). This finding was supported also by the results of photosynthetic pigment analysis, as the Chl *a*/*b* ratio significantly decreased in hybrid LYPJ rice during the later senescence process (Wang *et al.* 2014). The inactivation of RCs in hybrid LYPJ rice during the senescence stage was considered a downregulation mechanism in order to dissipate the excess of absorbed light (Holland *et al.* 2014, Kalaji *et al.* 2014). The dissipation indicators (φD_0, DI_0/RC, DI_0/CS_M) analyzed in this study also suggested that energy dissipation was enhanced in order to protect ageing leaves from photodamage (Table 2).

PI_{abs} is very sensitive to environmental stress and has been used to differentiate among cultivars for their responses to different abiotic stresses including natural senescence (Boureima *et al.* 2012, Holland *et al.* 2014, Kalaji *et al.* 2014). The decreased PI_{abs} during natural senescence process in hybrid LYPJ rice suggested that PSII function could be possibly altered by inducing a loss of electron transport capacity. This assumption was also supported by values of the relative driving force (DF) for photosynthesis and the relative electron transport activity (Fig. 4). PI_{tot} differed from PI_{abs} because it included PSI-related reactions (Stefanov *et al.* 2011). It allowed extending our knowledge of the photosynthetic electron transport activity beyond PSII and involving changes in the intersystem electron transport and PSI-related processes. The variation of PI_{abs} was more notable than that of $PI_{tot,}$ indicating the PSI was less affected than PSII. This is in agreement with the results obtained in *Quercus* during natural senescence (Holland *et al.* 2014). Moreover, the different experimental techniques for investigation of the primary targets could contribute to the controversial results in flag leaves during the senescence stage (Tang *et al.* 2005, Zhang *et al.* 2007).

Conclusion: From Chl *a* fluorescence analyses, we tentatively concluded that the inhibition of the electron transport in hybrid LYPJ rice caused by natural senescence might occur partly due to uncoupling of the OEC and/or inactivation of PSII reaction centers. The bigger part of the absorbed energy was dissipated as heat in order to protect the photosynthetic apparatus from photodamage during natural senescence. Nevertheless, a considerable reduction of the PSI electron transport activity was observed at the later senescence in hybrid LYPJ rice, confirming that natural senescence not only inhibited the OEC–PSII electron transport, but also significantly limited the PSII–PSI electron flow.

References

Alberta K.R., Mikkelsen T.N., Ro-Poulsen H.: Ambient UV-B radiation decreases photosynthesis in high arctic *Vaccinium uliginosum*. – Physiol. Plantarum **133**: 199-210, 2008.

Boureima S., Oukarroum A., Diouf M. *et al.*: Screening for drought tolerance in mutant germplasm of sesame (*Sesamum indicum*) probing by chlorophyll *a* fluorescence. – Environ.

Exp. Bot. **81**: 37-43, 2012.

Breštič M., Živčák M., Olšovská K. *et al.*: Reduced glutamine synthetase activity plays a role in control of photosynthetic responses to high light in barley leaves. – Plant Physiol. Biochem. **81**: 74-83, 2014.

Chen C., Chen H., Lin Y.S. *et al.*: A two-locus interaction causes interspecific hybrid weakness in rice. – Nat. Commun. **5**: 3357-3367, 2014.

Chhotaray D., Chandrakala Y., Mishra C.S.K. *et al.*: Farm practices influence the photosynthetic performance and plant efficiency of *Oryza sativa* L. – Acta Physiol. Plant. **36**: 1501-1511, 2014.

Ceppi M.G., Oukarroum A., Çiçek N. *et al.*: The IP amplitude of the fluorescence rise OJIP is sensitive to changes in the photosystem I content of leaves: a study on plants exposed to magnesium and sulfate deficiencies, drought stress and salt stress. – Physiol. Plantarum **144**: 277-288, 2012.

D'Amici G.M., Timperio A.M., Zolla L.: Coupling of native liquid phase electrofocusing and blue native polyacrylamide gel electrophoresis: a potent tool for native membrane multiprotein complex separation. – J. Proteome Res. **7**: 1326-1240, 2008.

Feng B., Liu P., Li G. *et al.*: Effect of heat stress on the photosynthetic characteristics in flag leaves at the grain-Filling stage of different heat-resistant winter wheat varieties. – J. Agro. Crop. Sci. **200**: 143-155, 2014.

Holland V., Koller S., Brüggemann W.: Insight into the photosynthetic apparatus in evergreen and deciduous European oaks during autumn senescence using OJIP fluorescence transient analysis. – Plant Biol. **16**: 801-808, 2014.

Hsu B.D.: On the possibility of using a chlorophyll fluorescence parameter as an indirect indicator for the growth of *Phalaenopsis* seedlings. – Plant Sci. **172**: 604-608, 2007.

Hussain M.I., Reigosa M.J.: A chlorophyll fluorescence analysis of photosynthetic efficiency, quantum yield and photon energy dissipation in PSII antennae of *Lactuca sativa* L. leaves exposed to cinnamic acid. – Plant Physiol. Biochem. **49**: 1290-1298, 2011.

Jiao D., Ji B., Li X.: Characteristics of chlorophyll fluorescence and membrane-lipid peroxidation during senescence of flag leaf in different cultivars of rice. – Photosynthetica **41**: 33-41, 2003.

Kalachanis D., Manetas Y.: Analysis of fast chlorophyll fluorescence rise (O-K-J-I-P) curves in green fruits indicates electron flow limitations at the donor side of PSII and the acceptor sides of both photosystems. – Physiol. Plantarum **139**: 313-323, 2010.

Kalaji H.M., Oukarroum A., Alexandrov V. *et al.*: Identification of nutrient deficiency in maize and tomato plants by in vivo chlorophyll a fluorescence measurements. – Plant Physiol. Biochem. **81**: 16-25, 2014.

Kreslavski V.D., Lankin A.V., Vasilyeva G.K. *et al.*: Effects of polyaromatic hydrocarbons on photosystem II activity in pea leaves. – Plant Physiol. Biochem. **81**: 135-142, 2014.

Kumar K.S., Dahms H.U., Lee J.S. *et al.*: Algal photosynthetic responses to toxic metals and herbicides assessed by chlorophyll a fluorescence. – Ecotoxicol. Environ. Safe. **104**: 51-71, 2014.

Kügler M., Jänsch L., Kruft V. *et al.*: Analysis of the chloroplast protein complexes by blue-native polyacrylamide gel electrophoresis (BN-PAGE). – Photosynth. Res. **53**: 35-44, 1997.

Lazár D.: The polyphasic chlorophyll a fluorescence rise measured under high intensity of exciting light. – Funct. Plant Biol. **33**: 9-30, 2006.

Lazár D., Nauš J.: Statistical properties of chlorophyll fluorescence induction parameters. – Photosynthetica **35**: 121-127, 1998.

Li X.M., Chen M.J., Li J. *et al.*: Effect of endophyte infection on chlorophyll a fluorescence in salinity stressed rice. – Biol. Plantarum **58**: 589-594, 2014.

Mohapatra P.K., Khillar R., Hansdah B. *et al.*: Photosynthetic and fluorescence responses of *Solanum melangena* L. to field application of dimethoate. – Ecotoxicol. Environ. Safe. **73**: 78-83, 2010.

Osório J., Osório M.L., Correia P.J. *et al.*: Chlorophyll fluorescence imaging as a tool to understand the impact of iron deficiency and resupply on photosynthetic performance of strawberry plants. – Sci. Hortic.-Amsterdam **165**: 148-155, 2014.

Panda D., Sarkar R.K.: Natural leaf senescence: probed by chlorophyll fluorescence, CO_2 photosynthetic rate and antioxidant enzyme activities during grain filling in different rice cultivars. – Physiol. Mol. Biol. Plants **19**: 43-51, 2013.

Pollastrini M., Holland V., Brüggemann W. *et al.*: Interactions and competition processes among tree species in young experimental mixed forests, assessed with chlorophyll fluorescence and leaf morphology. – Plant Biol. **16**: 323-331, 2014.

Qiu Z., Wang L., Zhou Q.: Effects of bisphenol A on growth, photosynthesis and chlorophyll fluorescence in above-ground organs of soybean seedlings. – Chemosphere **90**: 1274-1280, 2013.

Schansker G., Tóth S.Z., Strasser R.J.: Methylviologen and dibromothymoquinone treatments of pea leaves reveal the role of photosystem I in the Chl a fluorescence rise OJIP. – Biochim. Biophys. Acta **1706**: 250-261, 2005.

Sharma D.K., Fernández J.O., Rosenqvist E. *et al.*: Genotypic response of detached leaves versus intact plants for chlorophyll fluorescence parameters under high temperature stress in wheat. – J. Plant Physiol. **171**: 576-586, 2014.

Shen W.J., Chen G.X., Xu J.G. *et al.*: Overexpression of maize phospho*enol*pyruvate carboxylase improves drought tolerance in rice by stabilization the function and structure of thylakoid membrane. – Photosynthetica **53**: 436-446, 2015.

Stefanov D., Petkova V., Denev I.D.: Screening for heat tolerance in common bean (*Phaseolus vulgaris* L.) lines and cultivars using JIP-test. – Sci. Hortic.-Amsterdam **128**: 1-6, 2011.

Stirbet A., Govindjee: On the relation between the Kautsky effect (chlorophyll a fluorescence induction) and Photosystem II: Basics and applications of the OJIP fluorescence transient. – J. Photochem. Photobiol. B **104**: 236-257, 2011.

Strasser R.J., Srivastava A., Govindjee: Polyphasic chlorophyll a fluorescence transient in plants and cyanobacteria. – Photochem. Photobiol. **61**: 32-42, 1995.

Strasser B.J., Strasser R.J.: Measuring fast fluorescence transients to address environmental questions: The JIP-test. – In: Mathis P (ed.): Photosynthesis: from Light to Biosphere. Pp. 977-980. Kluwer Academic Publishers, Dordrecht 1995.

Tang Y.L., Wen X.G., Lu C.M.: Differential changes in degradation of chlorophyll-protein complexes of photosystem I and photosystem II during flag leaf senescence of rice. – Plant Physiol. Bioch. **43**: 193-201, 2005.

Timperio A.M., D'Amici G.M., Barta C. *et al.*: Proteomics, pigment composition, and organization of thylakoid membranes in iron-deficient spinach leaves. – J. Exp. Bot. **58**: 3695-3710, 2007.

Tsimilli-Michael M., Strasser R.J.: *In vivo* assessment of plants' vitality: applications in detecting and evaluating the impact of Mycorrhization on host plants. – In: Varma A. (ed.): Mycorrhiza: State of the Art, Genetics and Molecular Biology, Eco-function, Biotechnology, Eco-Physiology, Structure and Systematics (3rd edition). Pp. 679-703. Springer, Dordrecht 2008.

Wang G., Hao Z., Anken R.H. *et al.*: Effects of UV-B radiation on photosynthesis activity of *Wolffia arrhiza* as probed by chlorophyll fluorescence transients. – Adv. Space Res. **45**: 839-845, 2010a.

Wang L.J., Fan L., Loescher W. *et al.*: Salicylic acid alleviates decreases in photosynthesis under heat stress and accelerates recovery in grapevine leaves. – BMC Plant Biol. **10**: 34-43, 2010b.

Wang Y.W., Zhang J.J., Yu J. *et al.*: Photosynthetic changes of flag leaves during senescence stage in super high-yield hybrid rice LYPJ grown in field condition. – Plant Physiol. Bioch. **82**: 194-201, 2014.

Wu H.B., Wang B., Chen Y. *et al.*: Characterization and fine mapping of the rice premature senescence mutant *ospse1*. – Theor. Appl. Genet. **126**: 1897-1907, 2013.

Wu M., Wang P.Y., Sun L.G. *et al.*: Alleviation of cadmium toxicity by cerium in rice seedlings is related to improved photosynthesis, elevated antioxidant enzymes and decreased oxidative stress. – Plant Growth Regul. **74**: 251-260, 2014.

Xia J., Li Y., Zou D.: Effects of salinity stress on PSII in *Ulva lactuca* as probed by chlorophyll fluorescence measurements. – Aquat. Bot. **80**: 129-137, 2004.

Yu G.H., Li W., Yuan Z.Y. *et al.*: The effects of enhanced UV-B radiation on photosynthetic and biochemical activities in super-high-yield hybrid rice Liangyoupeijiu at the reproductive stage. – Photosynthetica **51**: 33-44, 2013.

Zhang C.J., Chu H.J., Chen G.X. *et al.*: Photosynthetic and biochemical activities in flag leaves of a newly developed super high-yield hybrid rice (*Oryza sativa*) and its parents during the reproductive stage. – J. Plant Res. **120**: 209-217, 2007.